Applied Energy 102 (2013) 1492–1503

Contents lists available at SciVerse ScienceDirect

Applied Energy

journal homepage: www.elsevier.com/locate/apenergy

Wind energy potential assessment considering the uncertainties due to limited data

Sungmoon Jung [a], O. Arda Vanli [b], Soon-Duck Kwon [c,*]

[a] Department of Civil and Environmental Engineering, Florida A&M University – Florida State University College of Engineering, Tallahassee, FL 32310, USA
[b] Department of Industrial and Manufacturing Engineering, Florida A&M University – Florida State University College of Engineering, Tallahassee, FL 32310, USA
[c] Department of Civil Engineering, Chonbuk National University, Chonju, Chonbuk 561-763, South Korea

HIGHLIGHTS

- We propose a new Bayesian approach for wind energy resource estimation.
- The approach systematically considers various types of uncertainties.
- For illustration, we studied measured wind speeds near Yeosu, Korea.
- The approach better models the uncertainties due to the limited amount of data.

ARTICLE INFO

Article history:
Received 8 April 2012
Received in revised form 15 August 2012
Accepted 5 September 2012
Available online 8 October 2012

Keywords:
Wind energy
Wind resource assessment
Annual energy production
Uncertainty analysis
Bayesian models

ABSTRACT

A new Bayesian approach is proposed to estimate the annual energy production (AEP) of a site where construction of wind turbines is considered. The approach uses long-term wind speeds of a nearby weather station and short-term wind speeds near the target site. Uncertainties exist due to the limited amount of data in the target site, in addition to the inherent uncertainties in the wind speed, the air density, the surface roughness exponent, and the power performance of the turbine. The proposed method systematically addresses these uncertainties and provides the distribution of the AEP. For illustration, we used the wind speed data near Yeosu, Korea, and the power performance curve of a 3 MW turbine. For the site and the turbine studied, the range given by the 95% confidence interval corresponded to 8.9% of the mean AEP, and the range given by the 99% confidence interval corresponded to 11.9% of the mean AEP. Benefits of using the Bayesian approach compared to the classical statistical inference was also illustrated with the case study. The proposed approach provides a more conservative estimation considering the uncertainties due to the limited amount of data. Distributions of parameters of the prediction model are also provided, which enables a more detailed analysis of the prediction.

1. Introduction

Wind energy potential assessment is an important first step before selecting a site to build wind turbines. The wind energy potential may refer to the potential of an entire nation or continent [1] or the potential of a specific location [2–8]. The potential assessment is differentiated from the forecasting because the former typically deals with the prediction of the annual energy production whereas the latter typically deals with the prediction for the next 24–72 h.

Unlike the forecasting problem where many researchers worked on the effect of the uncertainty (see [9–11] for extensive literature review), the literature on the uncertainty of the potential assessment is somewhat limited. However, the uncertainty analysis is important to reduce the discrepancy between the prediction and actual production, which can be quite significant. For example, Tindal et al. [12] analyzed a large database consisted of 156 wind farms of Europe and North America to compare energy predictions and actual production. The analysis of 510 wind farm years (of the 156 wind farms) showed that the average ratio of actual production to prediction was 93.3%. The authors identified the two most significant causes of the discrepancy as turbine availability and wind speed measurement quality.

The wind energy potential of a site is characterized using the estimated annual energy production (AEP). The AEP is sometimes roughly estimated using the mean wind speed only [13], but it is typically calculated using the measured power curve of a turbine and the wind speed distribution of the site. Uncertainties exist in both the power curve and the wind speed distribution. The international standard in estimating the AEP and evaluating the uncertainty is the IEC 61400-12-1 [14]. The IEC standard makes some assumptions for easier use in practice, which does not consider interaction of uncertainties. Bastide and Harding [15] discussed various sources of uncertainties such as the aerodynamic effects

* Corresponding author. Tel.: +82 63 270 2289; fax: +82 63 280 2421.
E-mail address: sdkwon@chonbuk.ac.kr (S.-D. Kwon).

0306-2619/$ - see front matter © 2012 Elsevier Ltd. All rights reserved.
http://dx.doi.org/10.1016/j.apenergy.2012.09.011

of monitoring tower and equipment on the air flow, data quality, simplistic wind shear extrapolation, wind flow modeling, and wind speed density function. The authors provided an estimated financial loss for a sample site due to these errors, but they did not consider the interaction of these errors and simply accumulated the errors. Fontaine and Armstrong [16] provided similar explanations along with the comparison of the deterministic (IEC) method and the Monte Carlo analysis. The authors also provided a case study of a wind farm located in Italy. A more systematic approach can be found in Lackner et al. [17], where a mathematical approach to combine independent sources of uncertainty was presented. The paper also recommended measuring of wind speeds at hub height to significantly reduce the uncertainty in the assessment. The authors in a subsequent paper demonstrated that even short-term hub height measurement can substantially improve the accuracy of the prediction [18]. Kwon [19] presented a systematic Monte Carlo approach, which to date is the most comprehensive method in dealing with the interaction of various sources of uncertainties.

In dealing with the uncertainties, most studies employed the probability density function that represents the randomness (ex: the normal distribution), and the parameters of the function (ex: the mean and the variance). Obviously, the accuracy of the energy potential assessment depends on the accuracy of the estimates of the parameters. However, it is not always easy to obtain accurate estimates of the parameters because of the limited availability of the data and the uncertainty in the model parameters reflect in low confidence in predictions of wind speed and energy potential. In addition to the parameter uncertainty, measurements of the wind speed are typically available from a nearby weather station, but the estimates of the parameters obtained from these measurements do not fully represent the wind speed of the target site, and this is usually reflected in a prediction bias. Correction algorithms exist to improve the prediction, which compensate for the inaccuracy by using additional short-term measurements from the target site [20]. These algorithms greatly improve the accuracy of the prediction, yet the amount of data for the short-term measurements is typically small so the issue of the limited availability of the data still remains.

Bayesian methods are used in statistics to deal with the uncertainties of the estimates of the parameters. The Bayesian approach offers two benefits compared to the classical statistics. The first benefit is that subjective judgments based on expert knowledge or indirect information is incorporated systematically with observed data ([21], p. 330). For example, consider a case where long-term measured wind speeds are available from a nearby weather station, but measurements at the target site are too limited to provide reliable statistics. However, suppose that an expert is able to estimate the statistics of the wind speed at the target site based on published literature that had similar site characteristics. In the Bayesian approach, the expert estimation is formulated as the *prior* probability, which is systematically updated as additional measurements become available, to provide the *posterior* probability.

The second benefit of Bayesian methods is the ability to separate uncontrollable uncertainties and controllable uncertainties. The uncertainties in the potential estimation come from different sources—the inherent variability in the wind such as the variability in the climate, wind profiles, wind shear, and turbulence [22], the uncertainties due to the processing of measured wind speeds [23], and the uncertainties due to the inexact nature of mathematical models, the site of measurement, and the limited size of data. These uncertainties may be grouped into two categories. The uncontrollable uncertainties are due to the inherent nature of the phenomena, which is beyond our control in modeling, while the controllable uncertainties are due to our choice of mathematical models, data collection, etc., which in the ideal situation can be eliminated by using a "perfect" approach. The uncontrollable uncertainties are termed as the *aleatory* (or, intrinsic) uncertainty, and the controllable uncertainties are termed as the *epistemic* (or, knowledge-based) uncertainty [24]. Although the elimination of the epistemic uncertainty is not practically possible, different nature of these uncertainties suggests that it will be informative and beneficial to separate these uncertainties, and the Bayesian approach offers the framework to do so.

In this paper, we will present a Bayesian approach to utilize these benefits in the wind energy potential assessment. To illustrate the use of the proposed approach, it will be applied to a sample site and be compared to a deterministic approach.

2. Wind speed measurements

Wind speeds used in this paper were collected at the Yeosu Weather Station, the Kwangyang Bay site, and the Yi Sun-sin Bridge site in Korea [19,25]. Fig. 1 is a satellite photo that shows the three sites.

The Yeosu Weather Station is the reference site where long-term wind speeds were measured. It is located at an urban area surrounded by hills (north and west), an island (southeast), and the sea (east and south). Hourly mean wind speeds between 1/1/1983 and 12/31/2007 were collected at the standard 10 m height. The Kwangyang Bay site is the target site where the wind energy potential was assessed. The distance between the Yeosu Weather Station and the Kwangyang Bay site is 16 km. There is a 500 m mountain between the Yeosu Weather Station and the Kwangyang Bay site. At Kwangyang Bay, hourly mean wind speeds between 1/1/2006 and 12/31/2006 were collected. The tower at Kwangyang Bay was 10 m high, but the anemometer was constructed at 2.5 m above the tower. The exposure of the tower within the 1 km radius is the sea. There are factories and storage facilities to the 2–3 km north and south of the tower, and hills to the 4–5 km east and west.

Since the tower at Kwangyang Bay was only 10 m high, data from the Yi Sun-sin Bridge site was also utilized to estimate wind speed at the hub height. The Yi Sun-sin Bridge site had a 60 m tower that recorded 10-min wind speeds at 10 m, 35 m, and 60 m, in order to provide data for designing a new bridge. The exposure is a combination of open water and factories to the south and the west, and open land and factories elsewhere. There is a 500 m mountain 4 km north of the tower. This research used wind

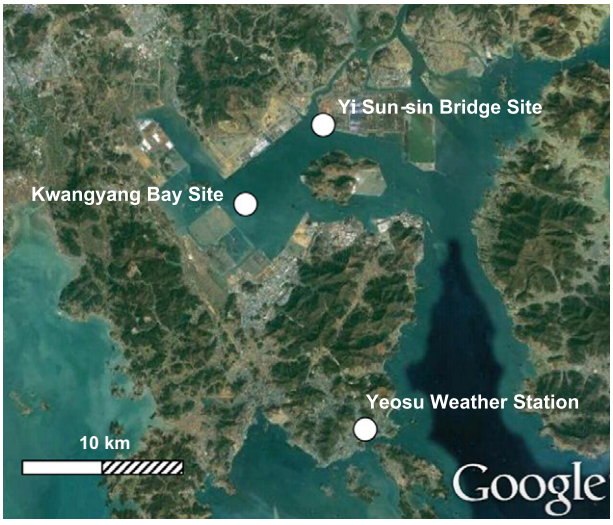

Fig. 1. Wind speed measurement sites.

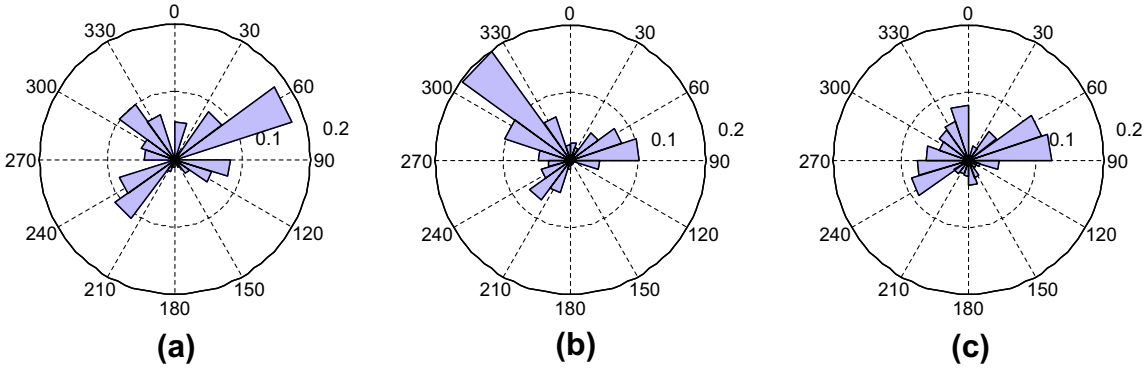

Fig. 2. Normalized histograms of the wind directions of the three sites: (a) Yeosu Weather Station, (b) Kwangyang Bay Site and (c) Yi Sun-sin Bridge Site.

speeds at 10 m and 60 m recorded between 8/1/2007 and 7/31/2008 in order to improve the accuracy of the potential assessment for the nearby Kwangyang Bay site. The distance between the Kwangyang Bay site and the Yi Sun-sin Bridge site is 6 km.

Two assumptions were made in using wind speeds from these sites. First, elevation difference between the Yeosu Weather Station (reference) and the Kwangyang Bay site (target) was ignored. The Yeosu Weather Station is located at a hill, which is 67 m from the sea level. Although wind speeds were measured at 10 m from the ground level of the Yeosu Weather Station, the elevation difference between the reference and the target may introduce some errors. Second, the surface roughness of the Kwangyang Bay site was assumed as similar to that of the Yi Sun-sin Bridge site. This assumption may introduce some errors because the distance between the two sites is 6 km, and also the surroundings of the two sites are somewhat different as shown in Fig. 1 and explained in previous paragraphs. To facilitate the understanding of relative contributions of the surroundings, normalized histograms of the wind directions are shown in Fig. 2. The data from 2006 was used for the Yeosu Weather Station and the Kwangyang Bay site. The data between 8/1/2007 and 7/31/2008 was used for the Yi Sun-sin Bridge site.

3. Deterministic approach without considering the uncertainties

In order to compare the performance of the proposed Bayesian approach (which will be introduced in Section 4 below), we will consider the traditional approach to calculate the annual energy production without accounting for uncertainties. The annual energy production (AEP) quantifies the wind energy potential of a given site. It is estimated by multiplying the total hours by the average wind turbine power.

$$E_{\mathrm{AEP}} = T\int_0^{\infty} P_{wt}(V) f_V(V)\,dV \tag{1}$$

in which T is the number of hours for one year, $P_{wt}(V)$ is the power performance curve, and $f_V(V)$ is the wind speed probability density function (PDF). The power performance curve $P_{wt}(V)$ is a single fixed curve. The power performance curve is typically obtained from the manufacturer of the turbine.

AEP estimated using Eq. (1) is based on the mean values of the power performance curve and the wind speed PDF therefore does not account for the uncertainties.

3.1. Wind speed PDF

To describe the distribution of the mean wind speed, the Weibull PDF is commonly used.

$$f_V(V) = \frac{k}{c}\left(\frac{V}{c}\right)^{k-1}\exp\left\{-\left(\frac{V}{c}\right)^{k}\right\} \tag{2}$$

in which V is the mean wind speed, k is the shape parameter, and c is the scale parameter. The parameters, based on the moment estimate method, are given by [26]:

$$\mu_k = \left(\frac{\sigma_V}{\mu_V}\right)^{-1.091} \tag{3}$$

$$\mu_c = \frac{\mu_V}{\Gamma(1+1/k)} \tag{4}$$

in which Γ is the Gamma function. Note that the mean of the shape parameter and the scale parameter is used when the uncertainties are ignored. For detailed studies on estimating Weibull parameters or using other models, refer to [27–29].

3.2. Estimation of the wind speed at the target site

In wind energy potential assessment, usually only short-term measurements are available for the target site where the turbine is going to be constructed. On the other hand, we often have access to long-term measurements at another reference site such as a weather station. Measure-correlate-predict (MCP) algorithms enable the prediction of long-term wind speed for the target site under this situation. The Variance Ratio Method [20] is expressed as:

$$\widehat{V}_t = (\mu_{V_t} - (\sigma_{V_t}/\sigma_{V_r})\mu_{V_r}) + (\sigma_{V_t}/\sigma_{V_r})V_r \tag{5}$$

in which $\widehat{V}_t$ is the predicted wind speed at the target site, V_r is the observed wind speed at the reference site, and μ_{V_t}, μ_{V_r}, σ_{V_t} and σ_{V_r} are the mean and the standard deviation of the two concurrent data sets at the target site and the reference site.

3.3. Height extrapolation

Due to the large size of modern turbines, the wind speed should be extrapolated to the hub height. Meteorologists typically use the logarithmic law to describe the vertical profile of the wind. For practical applications, the power law is often employed for its simplicity [30]. The power law is expressed as:

$$V(z_2) = V(z_1)\left(\frac{z_2}{z_1}\right)^{\alpha} \tag{6}$$

in which α is the surface roughness exponent dependent on the roughness of terrain, and z_1 and z_2 are the height above ground or sea level. When wind speed measurements at two different heights are available, the surface roughness can be computed using the

measurements. If wind speed measurements are not available, an expert opinion or design code [31] may be referred to.

Most literature provides single value of the roughness exponent for the given terrain. However, to describe the observed speeds adequately a variable exponent is necessary [32]. In addition to the conventional constant roughness exponent, the following two variable roughness models were also employed in the analyses. The first equation empirically scales the Justus equation [19]. The second equation is a generalized form of the first equation.

$$\mu_\alpha(V) = 5\tilde{\alpha}(0.37 - 0.0881\ln(V)) \tag{7}$$

$$\mu_\alpha(V) = \gamma_0 + \gamma_1 \ln(V) \tag{8}$$

in which $\tilde{\alpha}$ is the mean roughness exponent of the site, γ_0 and γ_1 are regression coefficients estimated from the given data.

3.4. Procedure to estimate the AEP

If long-term wind speeds at the hub height are available, then to estimate the AEP at the hub height the following procedure can be performed:

(1) Obtain the mean and the standard deviation of the long-term wind speeds.
(2) Compute the shape parameter and the scale parameter of the Weibull distribution using Eqs. (3) and (4).
(3) Estimate the AEP using Eqs. (1) and (2), and the power performance curve from the manufacturer.

A more common case is that long-term wind speeds are available from a nearby weather station and the long-term data have to be extrapolated to the target site and to the hub height, as shown in the flowchart in Fig. 3. In this case, the procedure to estimate the AEP is:

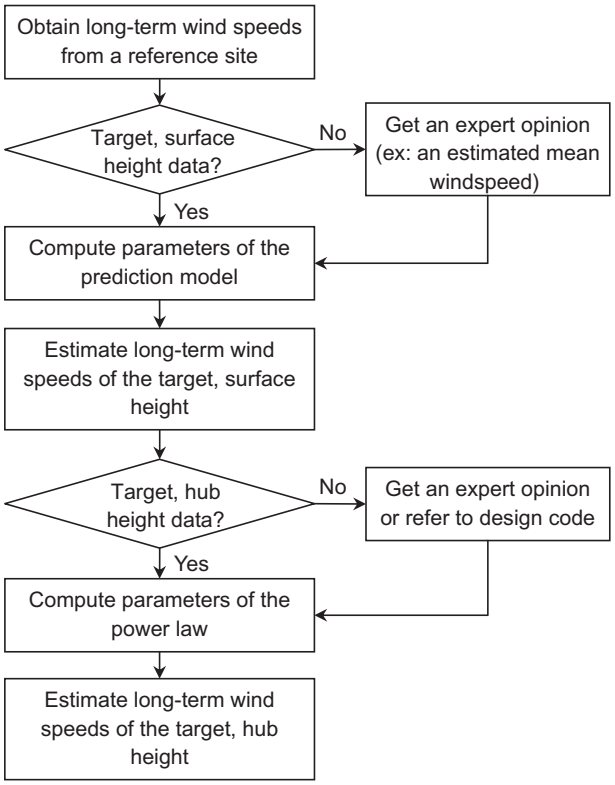

Fig. 3. Estimation of long-term wind speeds of the target site at the hub height, using the wind speed data from a reference site.

(1) Obtain the mean and the standard deviation of the wind speeds at the target site (surface height). If the data is not available, get an expert opinion to estimate the statistics.
(2) Obtain the mean and the standard deviation of the wind speeds at the reference site, using the data corresponding to the time period of step 1.
(3) Extrapolate the long-term wind speeds of the reference to the target using Eq. (5).
(4) Estimate the surface roughness exponent. If concurrent wind speeds at two different heights are available, use them to compute the exponent. If the data is not available, get an expert opinion or refer to the design code.
(5) Extrapolate the wind speeds of the surface height to the hub height using Eq. (6). Use Eqs. (7) and (8) if necessary.
(6) Obtain the wind speed PDF using Eqs. (2)–(4).
(7) Estimate the AEP using Eqs. (1) and (2), and the power performance curve from the manufacturer.

4. Proposed Bayesian approach to assess the AEP

In order to account for the effect of the uncertainties, we propose a Bayesian approach for the AEP calculation. The approach predicts the wind speed at the target site based on the historical data set. The predicted wind speeds are then used in the following discrete model to compute the wind turbine power and to obtain the AEP.

$$E_{\text{AEP}} = \sum_{j=1}^{T} P_{wt}(V_j)\tilde{\rho} \tag{9}$$

in which $\tilde{\rho}$ is the normalized air density from Eq. (10). Since the power performance curve $P_{wt}(V)$ is provided with respect to the standard air density of 1.225 kg/m^3, $\tilde{\rho}$ and the probability given in Eq. (10) will account for the uncertainties due to the change in the air density.

4.1. Air density

Energy potential equation is dependent on the air density. After analyzing actual measurements from Kwangyang Bay, a uniform (rectangular) probability distribution was used to represent the actual data [19]. Therefore, for Kwangyang Bay,

$$f_\rho = \begin{cases} \frac{1}{1.07-0.94} & (0.94 \leqslant \tilde{\rho} \leqslant 1.07) \\ 0 & (\textit{otherwise}) \end{cases} \tag{10}$$

in which $\tilde{\rho}$ is the air density normalized by the standard air density of 1.225 kg/m^3.

4.2. Power performance curve

To estimate the power output of a turbine, the power performance curve is necessary. The power performance curve shows power output under various wind speeds. It is provided by the manufacturer of the turbine. Standardized tests [14] are used to obtain the curve. Since the power performance curve only represents the average power output for given wind speeds, probability models are necessary to account for the uncertainty. In this research, the measured power performance curve of a wind turbine at Hangwon Windfarm in Jeju, Korea was used [33]. Based on the measurements, a normal distribution model for the power based on 10-min increment data had been developed in another paper [19], which was revised to be compatible with the hourly data used in this paper.

$$\sigma_{P_{wt}}(V) = \begin{cases} \left[-\frac{0.35(V-V_R)}{V_R-V_I} + 0.1\right]\mu_{P_{wt}}(V)/\sqrt{6} & (V_I \leqslant V \leqslant V_R) \\ 0.1\mu_{P_{wt}}(V)/\sqrt{6} & (V_R < V) \end{cases} \tag{11}$$

in which $\mu_{P_{wt}}(V)$ and $\sigma_{P_{wt}}(V)$ are the mean and the standard deviation of the power performance $P_{wt}(V)$, V_R is the rated wind speed of the turbine (15 m/s), and V_I is the cut-in wind speed of the turbine (4 m/s). The cut-out wind speed of the turbine used in this research is 25 m/s. Note that $\mu_{P_{wt}}(V)$ was provided by the manufacturer whereas Eq. (11) was developed using the measured power performance.

4.3. Uncertainty in the wind speed of the reference site

The Monte Carlo simulation and Eq. (9) require very long-term data (at least 100 years or longer) in order to simulate interactions of uncertainties on the AEP. If such data is available, it may be used directly in the simulation. If not, wind speed PDF needs to be defined using the wind speeds of the reference site, Eqs. (2)–(4), and the following. Then, wind speeds of any duration can be sampled from the PDF. Note that in this case, the uncertainty in the mean and the standard deviation is insignificant because the wind speed data at the reference site is long-term, and therefore, the Bayesian approach needs not be applied.

The dispersion of the shape parameter k depends on the length of the available data. The standard deviation of the shape parameter, obtained from the best fit of the available data is given by [19]:

$$\sigma_k = \mu_k \times 0.15 n_d^{-0.35} \tag{12}$$

in which n_d is the length of the data in months.

4.4. Estimation of the wind speed at the target site

In order to predict the wind speed at the target site as a function of the wind speed at the reference site (i.e., horizontal extrapolation) we will employ a Bayesian regression model. The model has V_t the wind speed at the target as the response and V_r the wind speed at the reference as the regressor as follows:

$$V_t = \beta_0 + \beta_1 V_r + e \tag{13}$$

in which e follows the normal distribution with zero mean and σ_e standard deviation. The regression parameters β_0 and β_1 are estimated in a Bayesian manner from a set of n observed wind speed data $V_{t1}\ldots V_{tn}$ at the target site and $V_{r1},\ldots,V_{rn}$ at the reference site. Suppose $\mathbf{V}_t$ and $\mathbf{V}_r$ (n by 1 vectors) are concurrent data sets at the target site and the reference site. Define $\mathbf{X} = [1 \quad \mathbf{V}_r]$ to be the n by 2 regressor matrix.

We assume noninformative prior distribution on the regression parameters as $p(\boldsymbol{\beta}, \sigma_e^2) \propto 1/\sigma_e^2$ where $\boldsymbol{\beta} = (\beta_0, \beta_1)$ is the vector of regression parameters. In Bayesian analysis, noninformative distributions are often employed when no prior knowledge about the model parameters β and σ_e^2 exist. Noninformative (also called flat or vague by some authors) priors assume that before observing any data all values of the parameters are equally likely [34].

The posterior distribution of the regression model parameters that correspond to noninformative priors and the assumed regression model Eq. (13) after observing the wind speed data at the reference and target locations are developed as follows. The posterior of the error variance follows an Inverse Gamma IG distribution [35]:

$$\sigma_e^2|\mathbf{V}_r, \mathbf{V}_t \sim IG((n-2)/2, s^2(n-2)/2) \tag{14}$$

In this notation $\sigma_e^2|\cdot$ denotes conditional or posterior distribution meaning that after observing the data $\mathbf{V}_r, \mathbf{V}_t$ the probability density of σ_e^2 is an inverse gamma. The shape and scale parameters of the distribution are $(n-2)/2$ and $s^2(n-2)/2$, respectively, where is the sample size and s^2 is the estimated error variance defined as:

$$s^2 = \frac{1}{n-k}(\mathbf{V}_t - \mathbf{X}\hat{\boldsymbol{\beta}})'(\mathbf{V}_t - \mathbf{X}\hat{\boldsymbol{\beta}}) \tag{15}$$

Note that the prime ($'$) denotes the transpose operation. The posterior of the regression coefficients is a multivariate normal distribution (MVN) with mean $\hat{\boldsymbol{\beta}}$ and variance–covariance matrix $\sigma_e^2(\mathbf{X}'\mathbf{X})^{-1}$:

$$\boldsymbol{\beta}|\mathbf{V}_r, \mathbf{V}_t, \ \sigma_e^2 \sim MVN(\tilde{\boldsymbol{\beta}}, \sigma_e^2(\mathbf{X}'\mathbf{X})^{-1}) \tag{16}$$

in which $\hat{\boldsymbol{\beta}} = (\mathbf{X}'\mathbf{X})^{-1}\mathbf{X}'\mathbf{V}_t$ is the vector of least squares estimates of the regression coefficients. The proposed approach obtains the predictions of the target wind speed by simulation. The posterior predictive distribution of the target wind speed is obtained as the integral:

$$p(V_t|\mathbf{V}_t) = \int p(V_t|\boldsymbol{\beta}, \sigma_e^2) p(\boldsymbol{\beta}, \sigma_e^2|\mathbf{V}_t) d\boldsymbol{\beta} d\sigma_e^2 \tag{17}$$

in which, by using the regression equation, the first quantity in the integral $p(V_t|\boldsymbol{\beta}, \sigma_e^2)$ is a normal distribution with mean $\beta_0 + \beta_1 V_r$ and variance σ_e^2 and the second quantity $p(\beta, \sigma_e^2|\mathbf{V}_t)$ is the posterior of the regression parameters. Samples from the predictive distribution can be drawn (without having to evaluate the integral) by simulation using the following algorithm:

(1) Draw error variance σ_e^2 from the posterior distribution $\sigma_e^2|\mathbf{V}_r, \mathbf{V}_t$ using Eq. (14).
(2) Conditional on σ_e^2, draw regression coefficients $\boldsymbol{\beta}$ using Eq. (16).
(3) Draw wind speed V_t at the target from $p(V_t|\boldsymbol{\beta}, \sigma_e^2)$.
(4) Go to step 1 and generate many samples.

4.5. Height extrapolation

The mean and standard deviation of surface roughness are assumed to be functions of the wind speed at the surface height by assuming the following relation:

$$\alpha(V_t) = \gamma_0 + \gamma_1 \ln V_t + \xi \tag{18}$$

in which γ_0 and γ_1 are unknown regression coefficients and ξ is model error. The model error is assumed to follow a normal distribution with mean 0 and standard deviation $\sigma_\xi \sigma_\alpha(V_t)$ which is the product of an unknown scale factor and σ_ξ a known standard deviation function

$$\sigma_\alpha(V_t) = 2.5\tilde{\alpha}\exp(-0.1V_t)(0.37 - 0.0881\ln(V_t)) \tag{19}$$

in which $\tilde{\alpha}$ is the mean roughness exponent of the site. The form reflects the observation that the standard deviation of the roughness exponent depends on the wind speed and the relation discussed in [19] was employed. Using the given data sets, the term σ_ξ will scale the assumed standard deviation.

The regression model parameters of the surface roughness are estimated using a Bayesian model from a set of n observations of hub height wind speed $\mathbf{V}_h = (V_{h1}, \ldots, V_{hn})$ and surface height wind speed $\mathbf{V}_t = (V_{t1}, \ldots, V_{tn})$. The relation between the surface and hub height wind speed can be given using the power law shown in Eq. (6). Note that $V(z_2) = V_h$ and $V(z_1) = V_t$. Therefore, the surface roughness can be estimated from the pairs of surface and hub height measurements. Let the n observations of the surface roughness obtained from above calculation be denoted by $\boldsymbol{\alpha} = (\alpha_1, \ldots, \alpha_n)$. Define $\mathbf{R} = [1 \quad \ln \mathbf{V}_t]$ to be the $(n \times 2)$ regressor matrix obtained from the logarithms of the surface height speeds $\ln \mathbf{V}_t$. According to model (18) the model errors follow a normal distribution but have unequal variances described by the variance covariance matrix $\sigma_\xi^2 \sum_\xi$ where the diagonal matrix:

$$\boldsymbol{\Sigma}_\xi = Diag(\sigma_\alpha^2(V_{t1}), \ldots, \sigma_\alpha^2(V_{tn})) \tag{20}$$

is the known variance covariance matrix and σ_ξ^2 is the unknown scale factor. The posterior of the scale factor is an inverse gamma distribution:

$$\sigma_\xi^2|\alpha \sim IG((n-2)/2, s_\xi^2(n-2)/2) \tag{21}$$

and the posterior of the regression coefficients $\boldsymbol{\gamma}$ is a multivariate normal distribution:

$$\boldsymbol{\gamma}|\sigma_\xi^2,\boldsymbol{\alpha} \sim MVN\left(\hat{\boldsymbol{\gamma}}, \sigma_\xi^2\left(\mathbf{R}'\sum\nolimits_z^{-1}\mathbf{R}\right)^{-1}\right) \tag{22}$$

in which $\hat{\boldsymbol{\gamma}} = (\mathbf{R}'\sum_z^{-1}\mathbf{R})^{-1}\mathbf{R}'\sum_z^{-1}\boldsymbol{\alpha}$ is the vector of weighted least squares estimates of the regression coefficients. The estimated error variance of the model is

$$s_\xi^2 = \frac{1}{n-k}(\boldsymbol{\alpha} - \mathbf{R}\hat{\boldsymbol{\gamma}})'\boldsymbol{\Sigma}_z^{-1}(\boldsymbol{\alpha} - \mathbf{R}\hat{\boldsymbol{\gamma}}) \tag{23}$$

Similar to the horizontal extrapolation, the predictions of hub height wind speed will be obtained by simulation:

(1) Draw error variance σ_ξ^2 from posterior distribution using Eq. (21).
(2) Conditional on σ_ξ^2, draw regression coefficients $\boldsymbol{\gamma}$ from the posterior using Eq. (22).
(3) Conditional on σ_ξ^2 and $\boldsymbol{\gamma}$ draw roughness exponent $\boldsymbol{\alpha}$ from:

$$p(\alpha|\boldsymbol{\gamma},\sigma_\xi^2) = N(\gamma_0 + \gamma_1 \ \ln V_t, \sigma_\xi^2\sigma_\alpha^2)$$

(4) Conditional on α, find wind speed at hub height $V_h = V_t(z_2/z_1)^\alpha$.
(5) Go to step 1 and generate many samples.

5. An illustrative example: the deterministic approach

This section analyzes the AEP using the conventional deterministic approach explained in Section 3. The deterministic approach uses the mean values of the wind speed PDF and the power performance curve. We will compare the results to the proposed Bayesian approach in Section 6.

First, concurrent wind speeds measured between 1/1/2006 and 12/31/2006 were used to obtain the MCP parameters. The mean and the standard deviation of the hourly wind speed at the target (Kwangyang Bay) was 4.426 and 2.916. The mean and the standard deviation of the hourly wind speed at the reference (Yeosu Weather Station) was 4.013 and 2.770. The slope of the obtained MCP equation was 1.053 and the y-intercept was 0.202.

Next, the roughness exponent was computed using the 10 m and 60 m wind speeds measured between 8/1/2007 and 7/31/2008 at the Yi Sun-sin Bridge site, which had similar surface characteristics to the target site. Since the anemometers at the Yi Sun-sin Bridge site reported 10-min wind speeds, they were first converted to hourly wind speeds so that the data among all sites are compatible. When all hourly speeds were used, 12.2% of hourly speeds produced unrealistic roughness exponents (smaller than zero or greater than one). These unrealistic exponents were excluded in computing the average roughness exponent. The computed average roughness exponent was 0.182, which was used in the constant roughness exponent and the variable roughness exponent model of Eq. (7). The data was also used to obtain the regression coefficients of Eq. (8), which were computed as $\gamma_0 = 0.2062$ and. $\gamma_1 = -0.0237$ Fig. 4 compares these roughness exponents obtained with constant and variable exponent models discussed in Section 3.3. Overall, Eq. (8) provided the best fit but it slightly underestimated the roughness exponent of higher speeds.

After obtaining the parameters for MCP and the roughness exponent, the long-term wind speeds at the reference between 1983 and 2007 were extrapolated to the target surface height (12.5 m) and then to the target hub height (80.0 m). Finally, the Weibull parameters were obtained and then the AEP was computed. Table 1 summarizes the obtained wind speed statistics and Weibull parameters. Fig. 5 graphically compares the wind speed PDFs at different stages. The AEP was computed as 6363 MW h for the constant roughness exponent, 6621 MW h for the variable roughness exponent using Eq. (7), and 5932 MW h for the variable roughness exponent using Eq. (8). Note that the AEP is different from what was reported in another paper [19] because in this paper new data was used to compute the surface roughness, which turned out to be higher than the earlier estimation. The roughness exponent had a significant impact on the AEP. If we take the AEP of the constant roughness model as 100% since the constant model is frequently used in practice, the AEP changed between 93% and 104% by selecting a different roughness exponent model.

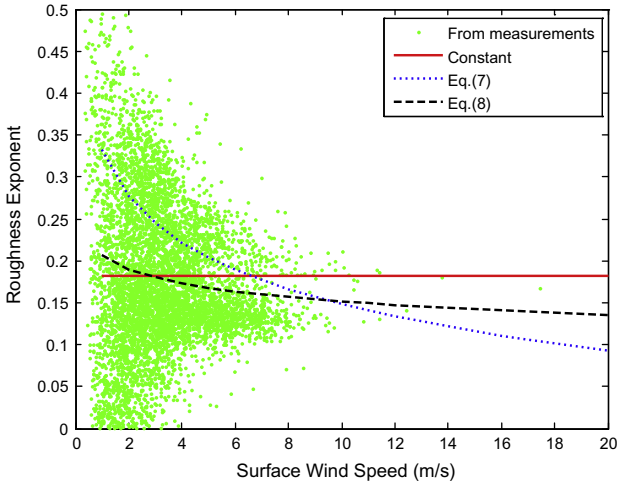

Fig. 4. Comparison of roughness exponents used in the deterministic analysis.

Table 1
Wind speed statistics and Weibull parameters in the deterministic analysis.

	Wind speed statistics		Weibull parameters	
	μ	σ	k	c
Reference measurement (1983–2007)	4.089	2.750	1.542	4.544
Reference measurement (2006)	4.013	2.770	1.498	4.445
Target measurement @ 12.5 m (2006)	4.426	2.916	1.577	4.930
Target estimated @ 12.5 m	4.506	2.895	1.620	5.031
Target estimated @ 80.0 m (constant roughness exponent)	6.315	4.057	1.621	7.051
Target estimated @ 80.0 m (variable roughness exponent, Eq. (7))	6.547	3.655	1.889	7.377
Target estimated @ 80.0 m (variable roughness exponent, Eq. (8))	6.131	3.787	1.692	6.869

6. An illustrative example: the proposed approach

6.1. AEP analysis using the proposed approach

The proposed approach considers the mean and the variance of the wind speed PDFs and the power performance curve. The interactions of the uncertainties at the stages of horizontal extrapolation, vertical extrapolation, and the wind turbine power calculation are considered using the procedure explained in Section 4.

The simulation was run for 1000 years. For each year of the simulation, $365 \times 24 = 8760$ hourly wind speeds were generated for the reference site using the Weibull distribution with the parameters shown in the first row of Table 1. The reason for using the Weibull distribution instead of the actual measurement was because the measurement was available for only 25 years whereas

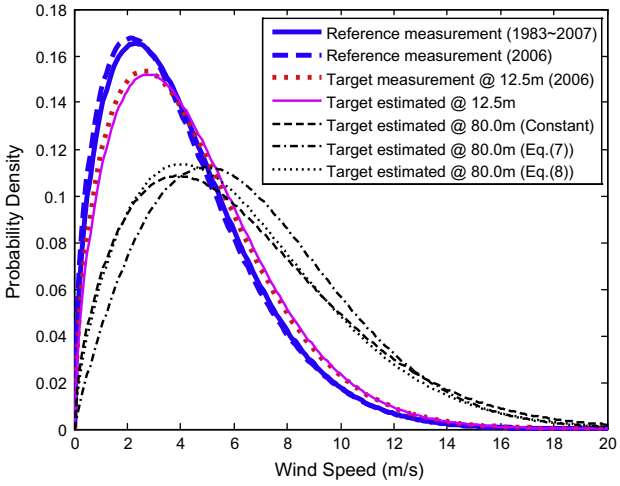

Fig. 5. PDFs of measured and estimated wind speeds in the deterministic analysis.

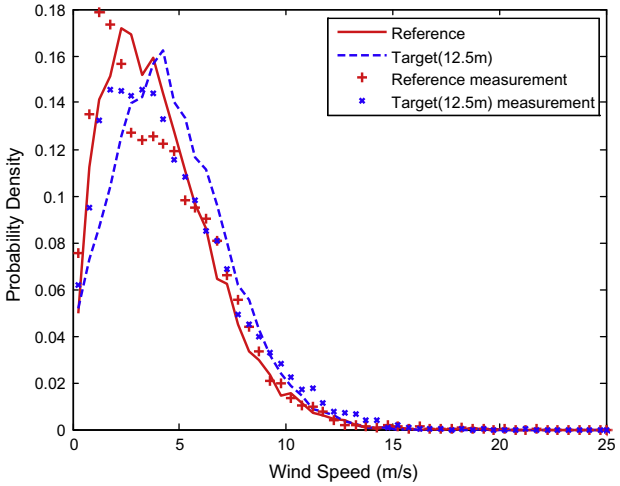

Fig. 7. Wind speeds at the reference and the target from the horizontal extrapolation: histogram of measurements vs. simulated data (lines are from the simulation year 1).

the simulation was done for 1000 years. Fig. 6 plots the histograms of generated wind speeds for all 1000 years. Compared to the histogram of actual measurements between 1983 and 2007, the wind speeds higher than 5 m/s were more accurate than the wind speeds lower than 5 m/s. This characteristic was favorable to the simulation because the cut-in speed of the turbine used in the simulation was 4 m/s and the lower wind speeds were ignored in the AEP calculation.

The next step was to apply the horizontal extrapolations of the hourly wind speeds using the procedure explained in Section 4.4. To obtain the predictive distributions, 1-year measured data at the reference and the target was used. Fig. 7 shows the histogram of simulated hourly wind speeds after the horizontal extrapolation. Only the simulation year 1 is shown for the clarity of the presentation. The solid and the dotted lines were obtained using the hourly speeds of the simulation year 1, so the lines changed for every year of the simulation reflecting the effect of the uncertainties. The figure clearly shows the deviation from the mean wind speed PDF shown in Fig. 5.

The vertical extrapolation is characterized by the roughness exponents. Fig. 8 compares values computed using the measured wind speeds, values generated during the simulation using the predictive distributions, and Eq. (7). The predictive distributions were

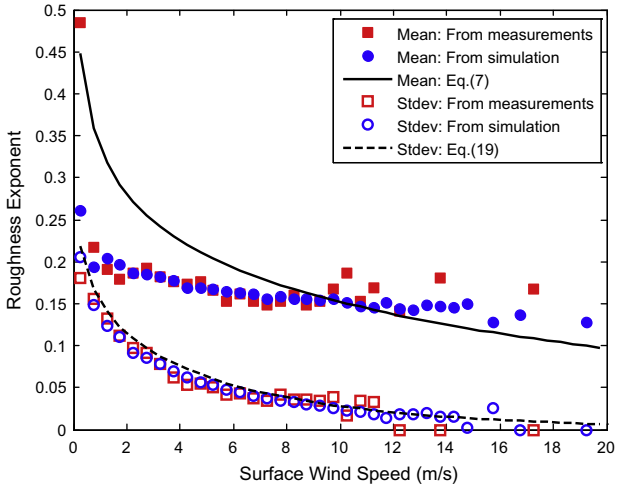

Fig. 8. Comparison of the roughness exponents obtained from the vertical extrapolation.

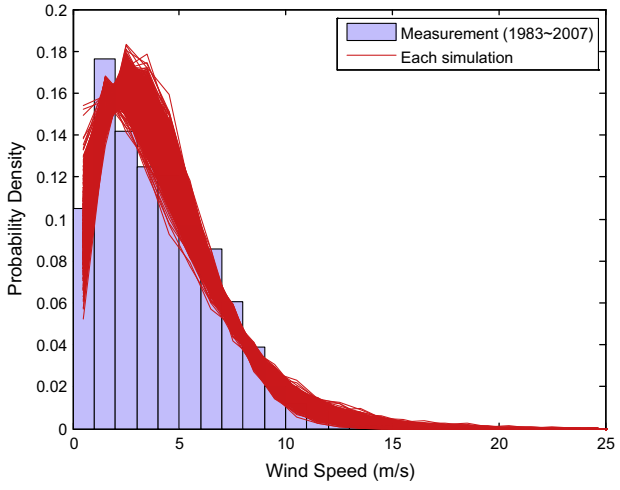

Fig. 6. Wind speeds at the reference: histogram of measurements vs. simulated data. Simulated values were obtained from the Weibull distribution.

calibrated using the 1-year data measured at 10 m and 60 m near the target site, using the procedure explained in Section 4.5. Eq. (7) showed an excellent fit for the site in Tjare [19], but the fit was not very good for the data used in this paper (square markers). On the other hand, the proposed approach calibrated the predictive distributions of the roughness exponent using the given data, and the mean of exponents generated during the simulation (circle markers) represented the actual measurements very well. In the previous research [19], Eq. (19) was obtained by scaling Eq. (7) to fit the Tjare data. Unlike the mean function, the standard deviation (Eq. (19)) showed an excellent fit for the standard deviation of the data used in this paper. The proposed simulation scales Eq. (19) using the given data, and it obviously also showed a good fit.

The importance of the roughness exponent was identified earlier in the deterministic analysis, so the roughness exponent of the uncertainty analysis was further analyzed. Fig. 9 compares the measured wind speeds and the simulated wind speeds obtained by applying the Bayesian approach at the wind turbine hub height. The advantage of the Bayesian approach can be seen in the figure when we compare the markers to the lines. The simulated wind speeds in the uncertainty analysis (circles) closely

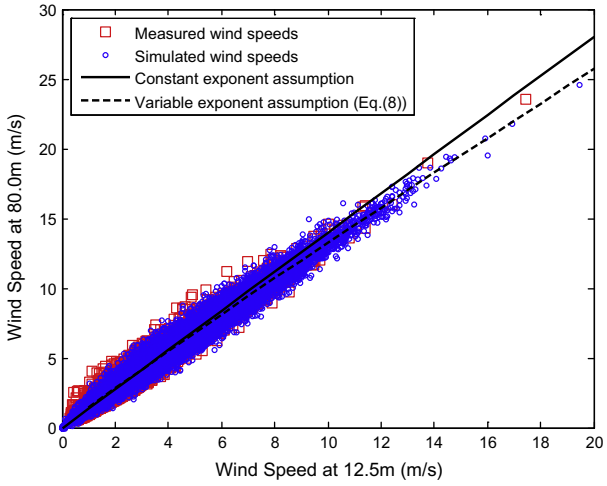

Fig. 9. Measured wind speeds vs. simulated wind speeds after applying the power law (circles are from simulation year 1).

follows the measured wind speeds (squares), both of which show scatters inherent in wind speeds. On the other hand, the deterministic analysis provides only point predictions resulting in lines shown in the figure. Therefore, the deterministic analysis is not able to quantify uncertainties inherent in the predictions. Overall, the simulated wind speeds match the measured wind speeds very well, especially up to the surface wind speed 13 m/s. However, the accuracy is not as good for the speeds of 14 m/s or higher due to the lack of the measured data. Only two records existed for the speeds higher than 14 m/s, which were not sufficient to change the predictive model. For the lower wind speeds up to 13 m/s, both the measured speeds and the simulated speeds follow Eq. (8). For the higher wind speeds, the measured speeds follow somewhere between the constant roughness assumption and the variable roughness assumption of Eq. (8), whereas the simulation follows primarily Eq. (8). Therefore, it is difficult to conclude that the real behavior follows only certain roughness model. In the following, the comparison of AEP of the uncertainty analysis and the deterministic analysis will show results from all roughness models.

The last step in the uncertainty analysis is to compute the AEP for the given simulation year using the predicted wind speeds at the hub height and the power performance curve. Fig. 10 shows example distributions of simulated wind speeds for the simulation year 1. The distributions were constructed from the histograms with bin width = 0.5 m/s. The distribution at 80 m shows higher wind speeds than the distribution at 12.5 m. It also shows more variability (the width of the distribution) than the distribution at 12.5 m. For a different simulation year, the histograms will change (see Fig. 6) reflecting the effects of the uncertainties, but the overall trends should remain the same. In the deterministic approach, only single curve was used to represent the wind speeds at the hub height as shown in Fig. 5. Fig. 11 shows simulated powers for the simulation year 1. For the same wind speed record, the power output in *y*-axis shows clearly the variations reflecting the uncertainty in the turbine power output. The variation of the power output increases for the increase in the wind speed up to 16 m/s. The trend would have continued if the number of simulated data points did not decrease for the higher speeds.

The AEP of each year of simulation will change due to the randomly generated uncertainties in the simulation. The simulation was repeated for 1000 years. The probability density of the AEP from the Bayesian approach (uncertainty analysis) is compared to the deterministic analysis results in Fig. 12. As explained earlier,

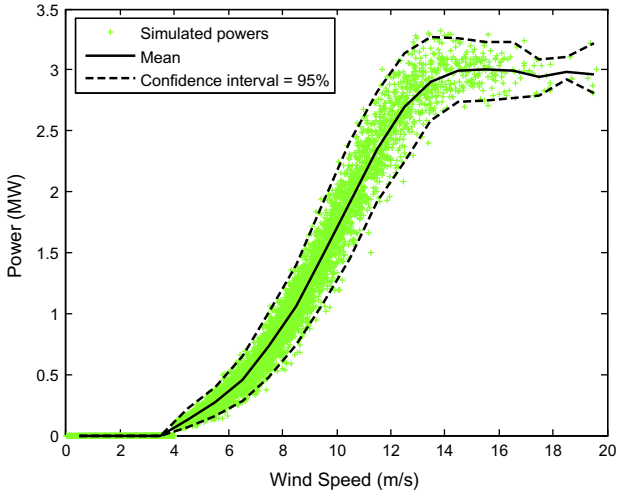

Fig. 11. Simulated powers for the simulation year 1.

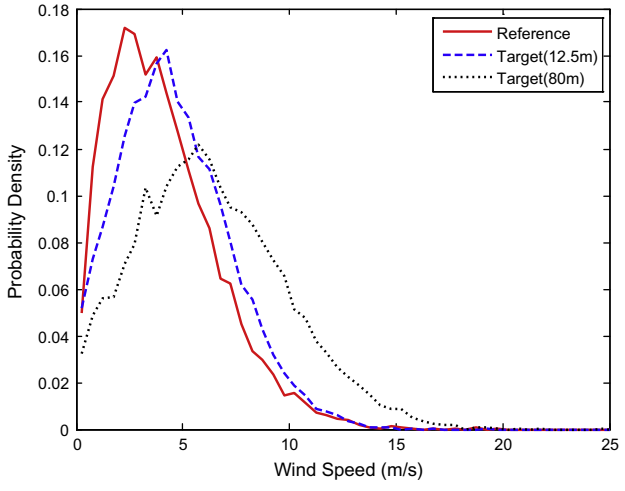

Fig. 10. Histogram of wind speeds obtained with the proposed Bayesian approach for the reference, the target at the surface height, and the target at the hub height (simulation year 1).

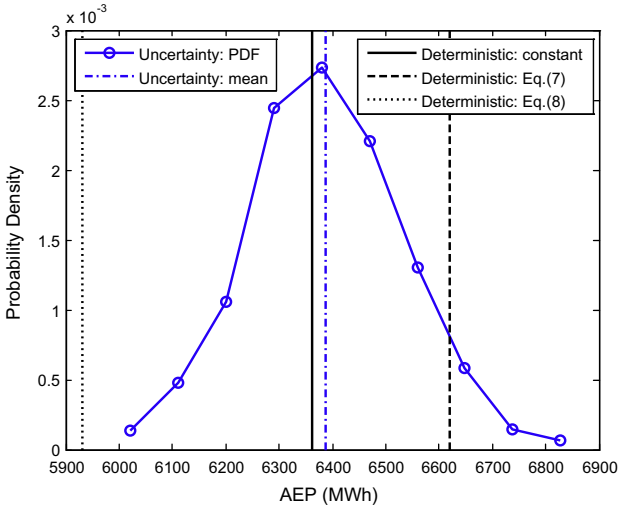

Fig. 12. Comparison of the probability density of the AEP obtained with the uncertainty analysis and the deterministic approach, using 1-year data.

it is not possible to state, for the site and the turbine analyzed in this paper, that certain roughness model was the most accurate, so the results from the uncertainty analysis were compared to all roughness models. When we take the mean of the uncertainty analysis as 100%, the AEPs from deterministic analyses with the constant roughness model, Eqs. (7) and (8) are 99.6%, 103.6%, and 92.9%, respectively. The limits obtained by the different roughness models are useful as lower or upper bounds on the energy production, but they are not able to quantify the probabilities. An advantage of the Bayesian approach evident from this Fig. 12 is that the PDF of the AEP enables us to more accurately calculate the probability that the AEP will lie in certain intervals. For example in Fig. 11 the probability that AEP is less than 6200 MW h can be estimated as about 16%. The deterministic analysis with the constant roughness model happened to be the closest to the mean of the uncertainty analysis (6388 MW h), but for another site the model may change based on an earlier study [19]. The 95 percentiles of the PDF are 6110 MW h and 6678 MW h, and the results from the constant roughness model and Eq. (7) are within the bound. The result from Eq. (8) is outside the bound, but the difference with respect to the lower bound is less than 3%. The 99 percentiles of the PDF are 6031 MW h and 6794 MW h, and the difference with respect to the lower bound becomes 1.6%. Therefore, we conclude that the PDF of AEP from the uncertainty analysis reasonably captures the results of deterministic analyses with various roughness models. Finally, the range given by the 95% confidence interval corresponds to 8.9% of the mean AEP. The range given by the 99% confidence interval corresponds to 11.9% of the mean AEP.

6.2. Comparison of Bayesian and frequentist approaches and effects of using short-term data

In order to study the benefits of the Bayesian approach we compare the uncertainty results to a traditional frequentist method. Bayesian inference considers all unknown parameters as random variables. Frequentist (classical) statistical inference considers population parameters as fixed but data as random due to sampling. Fig. 13 shows the Bayesian posterior distribution of the slope parameter β_1 and the error variance σ_e^2 from the horizontal extrapolation model using different data sizes.

The slope coefficient β_1 can be interpreted as the correlation between the reference and target wind speeds. As it can be seen in the posterior distributions, the parameter is more accurately estimated as more data points are used. The 95% confidence intervals of β_1 are as follows: with 1 week data 0.762 ∓ 0.111, with 1 month data 0.813 ∓ 0.049, and with 1 year data 0.776 ∓ 0.015, showing that the intervals become narrower with more data points. Therefore, for example, the prediction interval for target wind speed for a reference wind speed of 5 m/s (assume $\beta_0 = 1$) can be obtained using Eq. (13) as (4.26, 5.37) and (4.81, 4.96) with 1 week and 1 year data, respectively. Hence we capture the possibility that the wind speed can be as low as 4.26 m/s with 1 week data, but our minimum estimate with 1 year data will be 4.81 m/s. In addition, the posterior confidence interval of σ_e^2 that measures the model error are as follows: with 1 week data 4.769 ∓ 1.031, with 1 month data 4.066 ∓ 0.452, and with 1 year data 3.887 ∓ 0.119. Having a distribution for σ_e^2 rather than just single value (as we would have in a frequentist approach) accounts for additional uncertainty due to small sample size—the confidence interval with 1 week data is wider than 1 year data. This uncertainty is reflected in the posterior of the because the posterior of β_1 is generated conditional on the posterior of σ_e^2, as discussed in the simulation algorithm in Section 4.4.

Fig. 14 shows the posterior distribution of the slope parameter γ_1 and the error variance σ_ε^2 from the vertical extrapolation model. The slope γ_1 gives the relation between the log of the surface wind

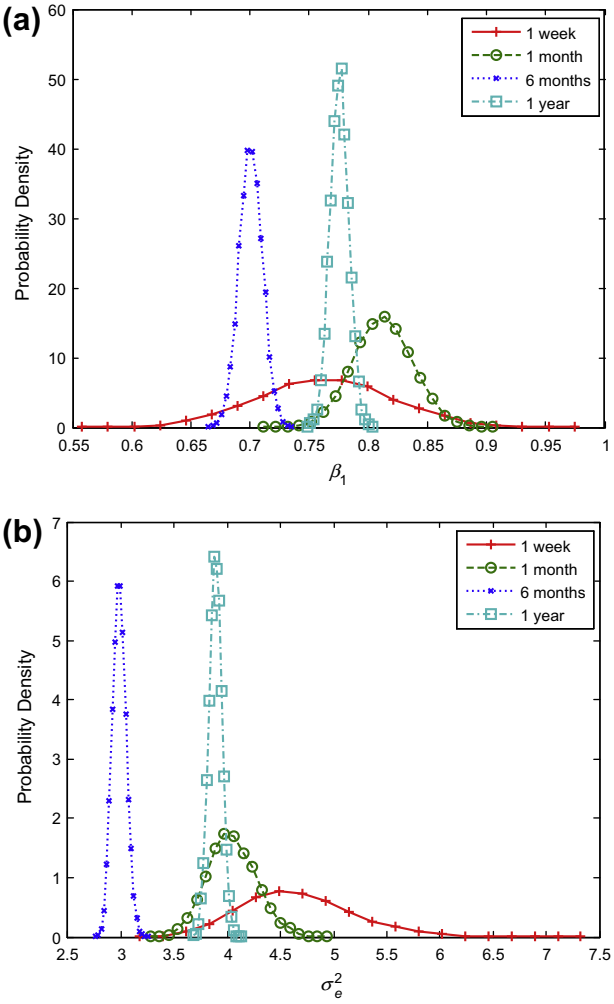

Fig. 13. Posterior distributions of the horizontal extrapolation model parameters: (a) β_1 and (b) σ_e^2.

speed and the roughness exponent through Eq. (18). The confidence intervals of γ_1 with 1 week and 1 year data are -0.018 ∓ 0.020 and -0.024 ∓ 0.0003. Therefore, for example, the surface roughness for a surface wind speed of 3 m/s (assume $\gamma_0 = 0.2$) can be predicted using Eq. (18) as (0.158, 0.202) and (0.170, 0.177) with 1 week and 1 year data, respectively. The effect of parameter uncertainty on the roughness exponent predictions is more completely illustrated in Fig. 15 which compares the roughness exponent predictions obtained by Eq. (18) for different surface wind speeds using two different data sizes 1 week and 1 year. The figure also plots the complete set of roughness exponents computed using measured wind speeds at 10 m and 60 m. As it can be seen, while the mean roughness estimates from both data sets are very similar, the prediction intervals from 1 year data more accurately captures the actual data (with wider prediction intervals) than 1 week data.

For the frequentist approach, we repeated the analysis outlined in Sections 4.4 and 4.5 by using the point estimates of the error variances rather than sampling from their posteriors (i.e. in step 1 we did not sample σ_e^2 but instead used the estimated value in step 2). It is important to note that for both approaches the distribution of power was the same in the last step of the uncertainty propagation, so the AEP results from two approaches are expected to be very similar. We repeated the analysis with the frequentist approach using the same 1 year data and simulated the posterior of AEP. Fig. 16 gives the posterior of AEP from the Bayesian

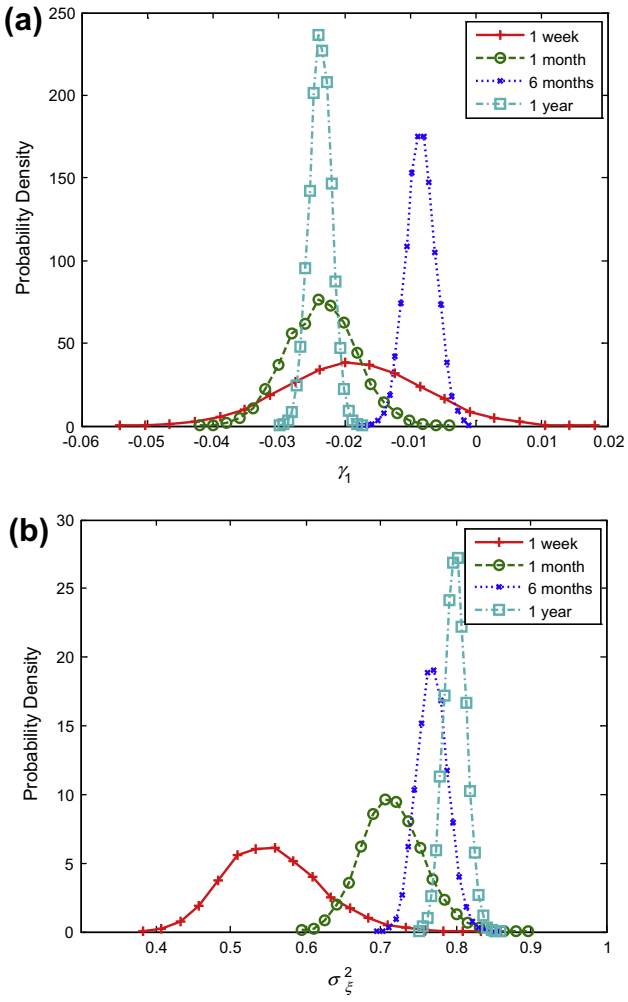

Fig. 14. Posterior distributions of the vertical extrapolation model parameters: (a) γ_1 and (b) σ_ξ^2.

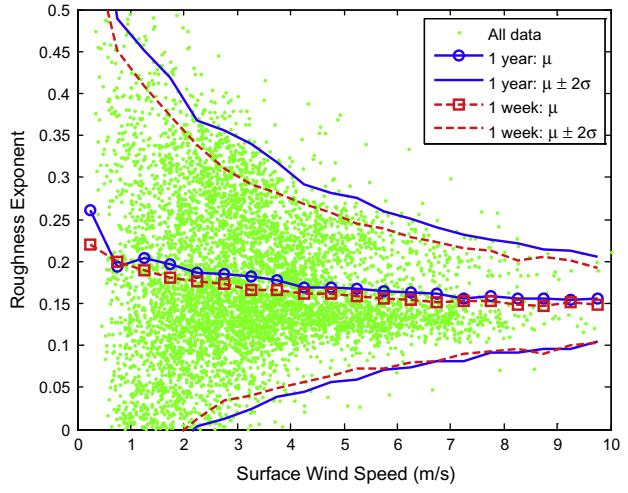

Fig. 15. Prediction interval of roughness exponent for different surface wind speeds: using the Bayesian approach (using 1 week and 1 year data).

approach and the simulated AEP distribution from the frequentist approach. The 99% prediction interval for AEP is obtained as (6031, 6794) MW h from the Bayesian approach while from the frequentist approach (6054, 6724) MW h. In the figure the

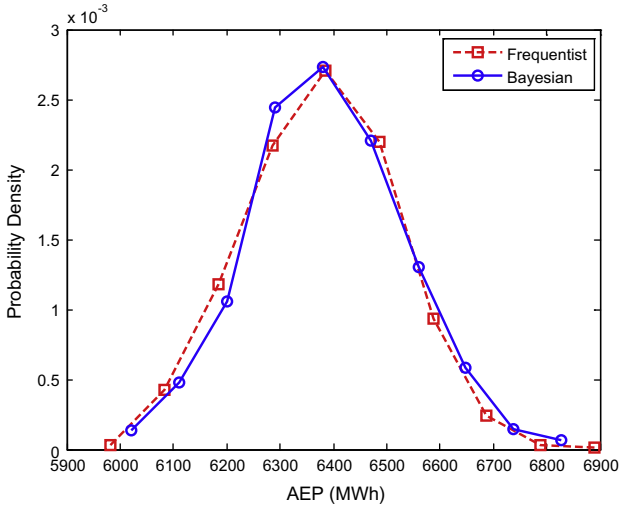

Fig. 16. Posterior distribution of the AEP from the Bayesian approach and the simulated AEP values using the frequentist approach.

frequentist approach seemingly shows wider estimation due to the outliers, but the 99 percentiles show that the lower bound of the Bayesian is 0.38% lower and the upper bound is 1.0% higher than the frequentist approach. The difference is because the Bayesian approach accounts for uncertainties due to sample size and parameter estimation and hence provides a wider bound on the energy potential estimate.

To better illustrate the capability of the Bayesian approach to account for additional uncertainties, one of the intermediate steps is explained below in detail. We will use the prediction of roughness exponent as an illustration, but other steps show similar behavior. We applied both the frequentist approach and the Bayesian approach to Eq. (18). Only 1-day data (April 1) was used for the clarity of the presentation. The 1-day data was used to obtain the parameters of Eq. (18). The frequentist approach then predicts the roughness exponent using single values of γ_0, γ_1, and σ_ξ, whereas the Bayesian approach treats these as random variables that have distributions. How both models predict the roughness exponent is compared in Fig. 17. Both models provide similar predictions, but it is clearly shown that the Bayesian approach provides a wider interval. When both models are compared to the

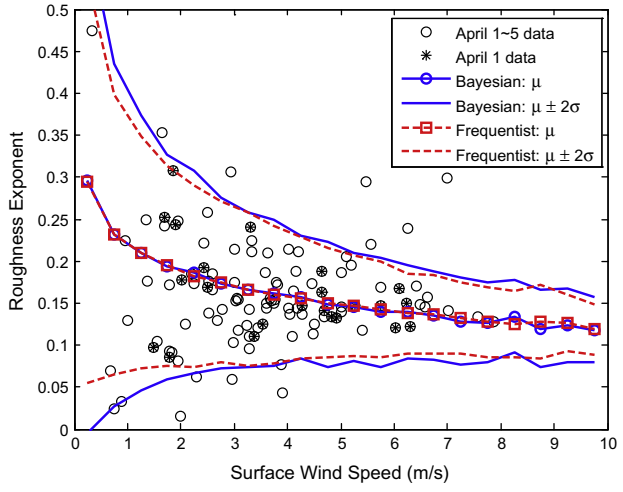

Fig. 17. Prediction interval of roughness exponent for different surface wind speeds: comparison of the Bayesian approach and the frequentist approach.

measured roughness exponent of the next 4 days (circle markers), the Bayesian approach better predicts the data not used in the estimation of the model parameters.

The proposed Bayesian approach opens a new possibility to use very short-term data (such as days) that conventionally was not sufficient to obtain the AEP reliably. The Bayesian approach enables us to overcome the uncertainties due to the limited amount of data. However, our attempts to predict the AEP using the very short-term data was not successful at this point due to another major challenge—daily, weekly, and seasonal variations of wind speeds that appeared to be greater than the uncertainties due to the limited amount of data. As explained in the introduction, that challenge belongs to a different category of uncertainty (aleatory) than the one addressed in this paper (epistemic). Further interdisciplinary research of this subject looks promising, such as collaboration between the engineering and the meteorology, but we leave it as a future study.

7. Summary and future work

We proposed a new Bayesian approach to estimate the annual energy production (AEP) of a site where construction of wind turbines is considered (termed as the target site). The approach uses long-term wind speeds of a nearby weather station (termed as the reference site), concurrent short-term wind speeds of the reference and the target, and concurrent short-term wind speeds at two different heights at the target. For illustration, we used 25 years of wind speeds at the Yeosu Weather Station and 1 year wind speeds at the Kwangyang Bay and Yi Sun-sin Bridge site. The following summarizes the conclusions of our investigations.

(1) When the conventional deterministic approach was used, the choice of the roughness exponent model significantly affected the AEP. The AEP changed between 93% and 104% by selecting a different roughness exponent model. The proposed approach reasonably captured the results of deterministic analyses above.
(2) For the site and the turbine studied, the constant roughness model of the deterministic analysis provided the closest match to the mean of the uncertainty analysis. When we took the mean of the uncertainty analysis as 100%, the AEPs from deterministic analysis with the constant roughness model was 99.6%.
(3) The proposed approach provides the AEP as the distribution rather than a point estimate. Therefore, the probability that the AEP will lie in certain intervals can be computed in the proposed approach.
(4) Compared to the frequentist (classical) statistical inference, the Bayesian approach treats the model parameters as random variables. The implication is that the Bayesian approach better considers the uncertainties due to the limited amount of data. For example, the prediction intervals from the Bayesian approach proved to be wider than those from the frequentist approach as shown in Figs. 16 and 17. Another advantage is that it provides distribution of parameters of the prediction model. For example, in addition to the correlation function between the reference wind speed and the target wind speed, expected errors in the prediction are also provided. Such information will be useful if the AEP needs to be predicted for another similar site where measurements are limited.

The focus of this paper was to present a new Bayesian approach in estimating the AEP. The following points were not fully addressed in this paper. They are recommended as future research topics.

(1) The proposed Bayesian approach opens a new possibility to use very short-term data (such as days) that conventionally was not sufficient to obtain the AEP reliably. However, additional studies are necessary to address daily, weekly, and seasonal variations in the AEP estimation.
(2) The current study computationally estimated the AEP for a hypothetical wind turbine. Its application on a real test case with measured AEP will provide valuable insight into the problem.
(3) The current study included only one case study. Its application on a different site with different topography and environmental conditions merits further research.
(4) We utilized the standard deviation functions from literature (Eqs. (11) and (19)) in both of the Bayesian and frequentist approaches. In a fully Bayesian approach the functions would also be estimated from data. The benefits of the Bayesian approach are expected to be more pronounced if these equations were estimated from data and the uncertainties of these coefficients were also included in the model. A possible extension of this research is to develop an experimental approach to include estimation of the standard deviation functions from the power and wind speed measurements.
(5) Another merit of the Bayesian approach over the frequentist approach is its ability to include prior information on the parameters in the form of prior distribution. Expert opinion on wind behavior can be incorporated into the statistical model in a formal way. In this study only noninformative prior distributions were employed. However, the proposed methodology provides a framework to include informative priors. Therefore, formulating appropriate priors from expert opinion and developing posterior distributions for informative priors could be investigated as a possible future study.

Acknowledgement

The third author was supported by the grant (11CCTI-A052604-04-000000) from the Ministry of Land, Transport and Maritime of Korean government through the Core Research Institute at Seoul National University for Core Engineering Technology Development of Super Long Span Bridge R&D Center.

References

[1] Elliott DL, Wendell LL, Gower GL. An assessment of the available windy land area and wind energy potential in the contiguous United States. Richland, Washington; 1991.
[2] Ramachandra TV, Subramanian DK, Joshi NV. Wind energy potential assessment in Uttara Kannada district of Karnataka, India. Renew Energy 1997;10(4):585–611.
[3] Rehman S, Ahmad A. Assessment of wind energy potential for coastal locations of the Kingdom of Saudi Arabia. Energy 2004;29(8):1105–15.
[4] Li M, Li X. Investigation of wind characteristics and assessment of wind energy potential for Waterloo Region, Canada. Energy Convers Manage 2005;46(18–19):3014–33.
[5] Bekele G, Palm B. Wind energy potential assessment at four typical locations in Ethiopia. Appl Energy 2009;86(3):388–96.
[6] Ucar A, Balo F. Evaluation of wind energy potential and electricity generation at six locations in Turkey. Appl Energy 2009;86(10):1864–72.
[7] Fyrippis I, Axaopoulos PJ, Panayiotou G. Wind energy potential assessment in Naxos Island, Greece. Appl Energy 2010;87(2):577–86.
[8] Akdağ SA, Güler Ö. Evaluation of wind energy investment interest and electricity generation cost analysis for Turkey. Appl Energy 2010;87(8):2574–80.
[9] Costa A, Crespo A, Navarro J, Lizcano G, Madsen H, Feitosa E. A review on the young history of the wind power short-term prediction. Renew Sust Energy Rev 2008;12(6):1725–44.
[10] Lei M, Shiyan L, Chuanwen J, Hongling L, Yan Z. A review on the forecasting of wind speed and generated power. Renew Sust Energy Rev 2009;13(4):915–20.
[11] Monteiro C, Bessa R, Miranda V, Botterud A, Wang J, Conzelmann G. Wind power forecasting: state-of-the-art 2009. Illinois: Argonne; 2009.

[12] Tindal A, Harman K, Johnson C, Schwarz A, Garrad A, Hassan G. Validation of GH energy and uncertainty predictions by comparison to actual production. In: AWEA wind resource and project energy assessment workshop. Portland; 2007.
[13] Fadare DA. The application of artificial neural networks to mapping of wind speed profile for energy application in Nigeria. Appl Energy 2010;87(3):934–42.
[14] IEC technical committee 88. IEC 61400-12-1. Wind turbines – Part 12–1: Power performance measurements of electricity producing wind turbines. Geneva, Switzerland: IEC; 2005.
[15] Bastide C, Harding J. Energy yield assessment – are you doing it right? In: EWEC2007, vol. 44. Milan; 2007.
[16] Fontaine A, Armstrong P. Uncertainty analysis in energy yield assessment. In: EWEC2007. Milan; 2007.
[17] Lackner MA, Rogers AL, Manwell JF. Uncertainty analysis in wind resource assessment and wind energy production estimation. In: 45th AIAA aerospace sciences meeting and exhibit. Reno, Nevada; 2007.
[18] Lackner MA, Rogers AL, Manwell JF, McGowan JG. A new method for improved hub height mean wind speed estimates using short-term hub height data. Renew Energy 2010;35(10):2340–7.
[19] Kwon S-D. Uncertainty analysis of wind energy potential assessment. Appl Energy 2010;87(3):856–65.
[20] Rogers AL, Rogers JW, Manwell JF. Comparison of the performance of four measure–correlate–predict algorithms. J Wind Eng Ind Aerodyn 2005;93(3): 243–64.
[21] Ang AH-S, Tang WH. Probability concepts in engineering planning and design. New York: John Wiley & Sons; 1975.
[22] Petersen EL, Mortensen NG, Landberg L, Hojstrup J, Frank HP. Wind power meteorology. Part I: Climate and turbulence. Wind Energy 1998;1: 2–22.
[23] Powell MD, Houston SH, Reinhold TA. Hurricane Andrew's landfall in South Florida. Part I: Standardizing measurements for documentation of surface wind fields. Weather Forecast 1996;11(3):304–28.
[24] Kiureghian AD, Ditlevsen O. Aleatory or epistemic? Does it matter? Struct Safety 2009;31(2):105–12.
[25] Kwon S-D, Lee SL. Estimation of design wind velocity based on short term measurements. KSCE J Civ Eng 2009;29:209–16.
[26] Carta JA, Ramírez P, Velázquez S. A review of wind speed probability distributions used in wind energy analysis: case studies in the Canary Islands. Renew Sust Energy Rev 2009;13(5):933–55.
[27] Chang TP. Performance comparison of six numerical methods in estimating Weibull parameters for wind energy application. Appl Energy 2011;88(1): 272–82.
[28] Chang TP. Estimation of wind energy potential using different probability density functions. Appl Energy 2011;88(5):1848–56.
[29] Celik AN, Kolhe M. Generalized feed-forward based method for wind energy prediction. Appl Energy 2012.
[30] Hsu SA, Meindl EA, Gilhousen DB. Determining the power-law wind-profile exponent under near-neutral stability conditions at sea. J Appl Meteorol 1994;33(6):757–65.
[31] ASCE 7-10. Minimum design loads for buildings and other structures. Reston (VA): American Society of Civil Engineers; 2010.
[32] Justus CG, Mikhail A. Height variation of wind speed and wind distributions statistics. Geophys Res Lett 1976;3(5):261–4.
[33] Kim K. Performance testing of Hang-won wind farm. J Korean Sol Energy Soc 2004;3(3):44–55.
[34] Press SJ. Subjective and objective Bayesian statistics. New York: John Wiley & Sons; 2003.
[35] Gelman A, Carlin JB, Stern HS, Rubin DB. Bayesian data analysis. Boca Raton, FL: Chapman & Hall/CRC Press; 2004.